Biophysical Chemistry 137 (2008) 76–80

Contents lists available at ScienceDirect

Biophysical Chemistry

journal homepage: http://www.elsevier.com/locate/biophyschem

A theoretical study of repeating sequence in HRP II: A combination of molecular dynamics simulations and ^{17}O quadrupole coupling tensors

Hadi Behzadi [a], Mehdi D. Esrafili [a], David van der spoel [b], Nasser L. Hadipour [a,c,*], Gholamabbas Parsafar [d]

[a] Department of Chemistry, Tarbiat Modares University, Tehran, Iran
[b] Department of Cell and Molecular Biology, Biomedical Centre, Box, 596, Uppsala University, SE-75 124 Uppsala, Sweden
[c] Institute of Chemistry, Academia Sinica, 128 Yen-Chiu - Yuan Rd. Nankang, Taipei 11529 Taiwan
[d] Department of Chemistry, Sharif University of Technology, Tehran, Iran

ARTICLE INFO

Article history:
Received 28 April 2008
Received in revised form 8 July 2008
Accepted 12 July 2008
Available online 22 July 2008

Keywords:
Nuclear quadrupole resonance
Density functional theory
Histidine rich protein II
MD simulations
Hydrogen bond

ABSTRACT

Histidine rich protein II derived peptide (HRP II 169–182) was investigated by molecular dynamics, MD, simulation and ^{17}O electric field gradient, EFG, tensor calculations. MD simulation was performed in water at 300 K with α-helix initial structure. It was found that peptide loses its initial α-helix structure rapidly and is converted to random coil and bent secondary structures. To understand how peptide structure affects EFG tensors, initial structure and final conformations resulting from MD simulations were used to calculate ^{17}O EFG tensors of backbone carbonyl oxygens. Calculations were performed using B3LYP method and 6–31+G* basis set. Calculated ^{17}O EFG tensors were used to evaluate quadrupole coupling constants, *QCC*, and asymmetry parameters, η_Q. Difference between the calculated *QCC* and η_Q values revealed how hydrogen-bonding interactions affect EFG tensors at the sites of each oxygen nucleus.

1. Introduction

One of the most important goals of modern biochemistry is to understand protein function through structural and dynamics studies. Although accurate determination of proteins conformation is a formidable task, it is crucial to effectively manipulate and change its function. Study of small peptide can also be helpful to understand protein structures. In biomacromolecules such as peptides, proteins, and carbohydrates, carbonyl oxygen plays a key role in molecular conformations, for instance through hydrogen bonding [1].

Oxygen-17 is a quadrupolar nucleus with nuclear spin angular momentum of $I=5/2$ and electric quadrupole moment, eQ, which interacts with electric field gradient, EFG, tensors. The interaction energy of EFG tensors and eQ is known as quadrupole coupling constant, C_Q, which can be measured experimentally by nuclear quadrupole resonance, NQR, spectroscopy [2–3]. As a result of hydrogen hydrogen-bonding formation in peptides, the resonating carbonyl oxygen-17 nucleus feels the changes in EFG, which is reflected as a shift in the NQR spectrum. Calculation of C_Q and its associated asymmetry parameter, η_Q, is performed via extracting the NQR frequencies, γ_Q.

Molecular dynamics (MD) simulation considers small size systems, at a typical scale of a few nanometers, and investigates the time evaluation of molecular system by computation of the interactions between their components [4,5]. MD simulations has been widely applied to biological macromolecules, such as proteins and peptides, to gain insight their dynamics, for studies of folding/unfolding, to compute free energy, and to investigate structure–function relationships [6–11]. MD simulation has provided detailed information on the fluctuation and conformational changes of proteins and peptides. For instance, MD simulations have used to investigate the conformational behavior of PrP 106–126 (PrP = prion protein) peptide [12,13].

In this study, MD simulation in combination with the calculation of NQR parameters are used in order to study of repeating sequence in malaria *Plasmodium falciparum* HRP II protein. HRP II is an extra-ordinary protein which consists mainly of three amino acids: histidine (34%), alanine (37%) and aspartic acid (10%) [14]. The most repeated sequence of HRP II is AHH, AHHAAD, and HHAHHAAD; however, the exact structure of this protein is not completely known. There is one theoretical model available in the protein data bank which indicates that HRP II is mainly composed of 18 α-helix regions [15]. However, circular dichroism (CD) spectroscopy measurements reveal that HRP II exists mainly as a random coil conformation in aqueous solution [16]. Pandey et al. [17] have shown that HRP II repeating sequences contain binding sites for heme enabling hemozoin formation and thereby detoxifying the toxic heme group in life cycle of malaria. In this paper, a 14 amino acid fragment of this protein, HRP II 169–182, with HHAHHAADAHHAAD sequence is studied (Fig. 1). This sequence contains two hexapeptide repeating units with α-helix structure. As the first step, a MD simulation is carried out to examine the conformational transitions. The results reveal that the predominant

* Corresponding author. Department of Chemistry, Tarbiat Modares University, Tehran, Iran. Tel.: +98 2188011001 3495; fax: +98 218800-9730.
E-mail address: hadipour@modares.com (N.L. Hadipour).

0301-4622/$ – see front matter © 2008 Elsevier B.V. All rights reserved.
doi:10.1016/j.bpc.2008.07.006

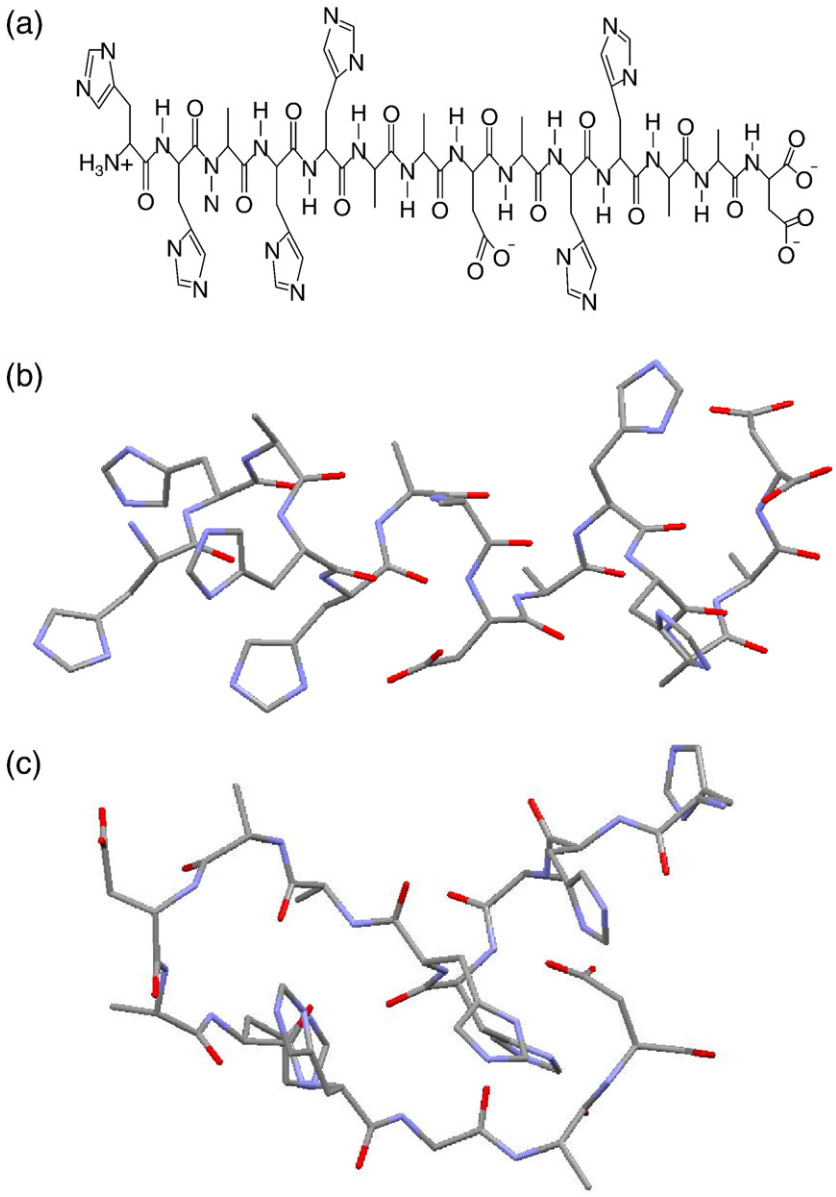

Fig. 1. (a) Chemical structure of HRP II 169–182 (HHAHHAADAHHAAD) peptide. (b) Initial conformation and (c) final MD conformation.

secondary structure of these peptides in solution is coil and bend. In addition to MD study, quantum chemical calculations are carried out to explore the influence of peptide conformation on ^{17}O EFG tensors of backbone oxygen nuclei. For this purpose, density functional theory (DFT) calculations are performed on initial α-helix structure and final coil and bend conformations obtained by MD simulations.

It is well recognized that determining the strength and geometry of HBs is a challenge for both experimental and theoretical studies. Regarding theoretical works, *ab initio* methods accounting for electron correlation are needed for an accurate description of HBs. Therefore Hartree–Fock calculations are not applicable to such situations. Also large enough basis sets are necessary to expand the wave function [18]. Thus, to make an accurate description of hydrogen bonded system with *ab initio* correlated methods together with high quality basis sets is really demanding. DFT, is widely used in computational chemistry due to its excellent performance-to-cost ratio. There are many flavors of approximations to $E_{XC}[\rho]$ in use today. Various studies reveal that the generalized gradient approximations (GGA) and hybrid functional are more accurate than local-density approximations (LDA) to describe the HBs [18,19–22].

DFT is currently the most popular electronic structure method. In spite of the known deficiency of DFT to describe the dispersion energy, it offers many advantages. The long-range dispersion interaction between two molecules cannot be described well with the standard used approximate density functionals. However, the dispersion

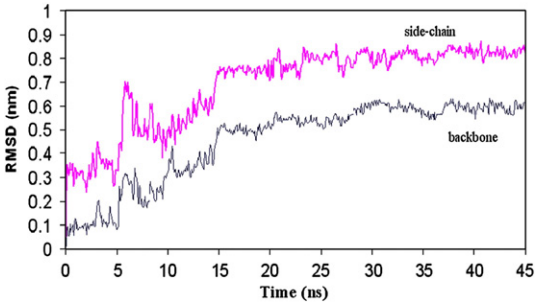

Fig. 2. Time dependence of root mean square deviation (RMSD) of backbone and side chain helix starting structure for HRP II 169–182 peptides during the molecular dynamic simulation.

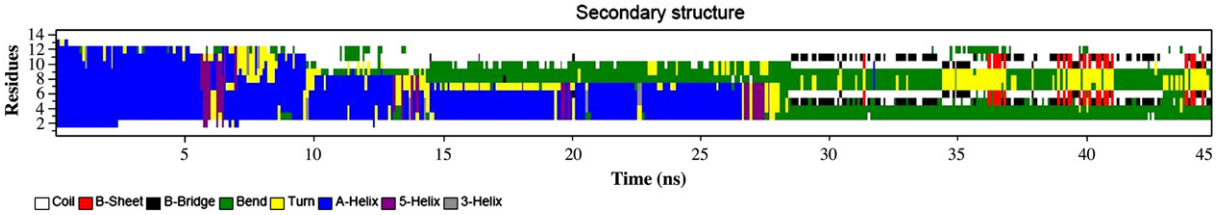

Fig. 3. Secondary structure of the HRP II 169–182 peptides as a function of simulation time.

coefficients which describe the interactions can be calculated well with DFT response calculations [23]. In this paper, we focused on properties that require information of one electronic state at a single point on the potential energy surface which are the electric field gradient as first order properties. Various DFT studies of electric [24], magnetic [25], and electromagnetic [26–28] linear response properties indicate that the B3LYP functional performs better than BLYP.

2. Computational details

2.1. Molecular dynamics simulations

Initial coordinates of peptide were taken from modeled structure of HRP II 169–182 in protein data bank (PDB entry 1L8M). The peptide consists of three residues types; alanine, histidine and aspartic acid (Fig. 1). The peptide was firstly put into a suitable sized simulation dodecahedron box and solvated with 2876 simple point charge (SPC) water model. Histidine and aspartic acid residues are neutral and negatively charged respectively and two Na^+ counter ions neutralize the negative charge. The solvated configuration energy was then minimized via steepest descent method and so obtained configuration was submitted to restrain MD simulation, keeping the peptide fixed. Finally, MD simulation was carried out at 300 K and 1 bar, NPT ensemble, for 45 ns [29]. Temperature and pressure were controlled by using Berendsen's temperature and pressure coupling methods [30]. The time step was 4 fs and LINCS used to constrain bond length [31–33]. We used a cut-off 14 Å for van der Waals interactions and particle-mesh-ewald (PME) method was used for the electrostatic interactions with a cut-off of 9 Å [34]. The GROMACS package [35] with the GROMOS96 force field [36] was employed for the simulation.

2.2. ^{17}O quadrupole coupling constants calculations

Quantum chemical calculations were performed to calculate the EFG tensors at the sites of ^{17}O nuclei using Gaussian 98 package [37] at the level of DFT. B3LYP functional method was employed in the EFG tensors calculations [38–40]. The EFG tensors were calculated at the level of 6–31+G* and SVP of Ahlrichs and coworkers basis sets [41]. The principal components of the EFG tensor, q_{ii}, are computed in atomic unit (1 au=9.717365×10^{21} V m^{-2}), with $|q_{zz}|\geq|q_{yy}|\geq|q_{xx}|$ and $q_{xx}+q_{yy}+q_{zz}=0$. These diagonal elements relate to each other by the asymmetry parameter: $\eta_Q=\frac{|q_{yy}-q_{xx}|}{|q_{zz}|}$, $0\leq\eta_Q\leq1$, that measures the deviation of EFG tensor from axial symmetry. The computed q_{zz} component of EFG tensor is used to obtain the nuclear quadrupole coupling constant from the equation; $C_Q\,(\mathrm{MHz})=\frac{e^2Qq_{zz}}{h}$ [42], where the standard value of $eQ(^{17}O)$ reported by Pyykkö is employed [43]: $eQ(^{17}O)$=25.56×10^{-28} m^2 and h is Planck's constant.

Table 1
The values of HB structural parameters for initial α-helix and final structures

Initial conformation			
Donor…acceptor	R(O…N)/Å	Donor…acceptor	O…H–N/deg
OHis2…NAla6	2.81	OHis2…H–N Ala6	152.01
OAla3…NAla7	2.98	OAla3…H–N Ala7	157.59
OHis4…NAsp8	2.95	OHis4…H–N Asp8	143.14
OHis5…NAla9	2.84	OHis5…H–N Ala9	156.97
OAla6…NHis10	2.97	OAla6…H–N His10	144.65
OAla7…NHis11	3.08	OAla7…H–N His11	159.06
OAsp8…NAla12	3.18	OAsp8…H–N Ala12	155.98
OAla9…NAla13	2.98	OAla9…H–N Ala13	174.97
Final conformation			
Donor…acceptor	R(O…N)/Å	Donor…acceptor	∠O…H–N/deg
OAla6…$C_{imidazol}$His11	2.85	OAla6…H–$C_{imidazol}$His11	119.59
OAla6…$N_{imidazol}$His11	3.02	OAla6…H–$N_{imidazol}$His11	104.54
OAla7…NAla9	3.13	OAla7…NHAla9	142.64
OHis10…NAla6	2.79	OHis10…H–NAla6	158.84
OAla13…$N_{imdazol}$His4	2.99	OAla13…H–N_{imi}His4	134.23

3. Results and discussion

Two techniques of MD simulations and ^{17}O EFG calculations were employed to theoretically study the repeating sequence of malaria protein, HRP II 169–182 peptide. The obtained results will be discussed in two separate sections.

3.1. Molecular dynamics simulation

Our main purpose is to understand how HRP II 169–182 α-helix peptide changes during simulation in water. Hence, the peptide corresponding to residues 169–182 of the HRP II protein was simulated starting from an α-helix conformation, for 45 ns. Fig. 2 shows root mean square deviation (RMSD) of side chain and backbone atoms from the initial α-helix HRP II 169–182 peptide. While proceeding from 5 to 28 ns, RMSD of backbone and side chain atoms increases progressively due to degradation of helix to coil and turn secondary structures, as shown by DSSP analysis [44] (Figs. 2, 3). After about 28 ns, RMSD fluctuation about 0.6 nm and 0.8 nm is found for backbone and side chain respectively as a result of peptide unfolding. This finding is in complete accordance with DSSP analysis after 30 ns indicating that peptide residues adopt random coil structure (49%), specifically in near C-terminal and N-terminal, while middle residues take bend structure (31%). These CBC (coil–bend–coil) conformations start after about 28 ns and are maintained through the rest of the simulation. After about 6 ns of simulation, the α-helix content of peptide begins to decrease and coil population increases. In the α-helix structure each carbonyl group CO (i) interacts with NH (i+4) through hydrogen bonding, where i is the residue number (Table 1). Evaluation of average i, i+4 hydrogen bond lengths is presented in Fig. 4. The HB distance is about 0.29 nm at the beginning of the simulation and remains nearly

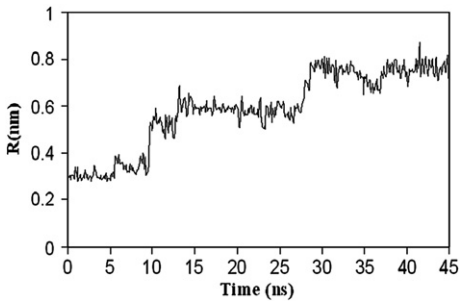

Fig. 4. Average i, i+4 hydrogen bond lengths during the simulation.

Table 2
Calculated ^{17}O EFG tensor (B3LYP/6–31+G*) and related converted NQR parameters for His, Ala and Asp residues in initial α-helix and final MD structure of HRP II 169–181(A and B refer to residue and secondary structure, respectively)

Initial α-helix conformation						Final configuration from MD simulation					
A	q_{xx}	q_{yy}	q_{zz}	C_Q	η_Q	B	q_{xx}	q_{yy}	q_{zz}	C_Q	η_Q
O–His1	−0.58 (−0.60)	−0.88 (−0.98)	1.46 (1.58)	8.78 (9.49)	0.21 (0.24)	Coil	−0.64 (−0.66)	−0.91 (−0.95)	1.55 (1.60)	9.32 (9.65)	0.17 (0.18)
O–His2	−0.63 (−0.65)	−0.85 (−0.95)	1.49 (1.61)	8.96 (9.66)	0.15 (0.19)	Coil	−0.66 (−0.69)	−0.84 (−0.91)	1.5 (1.60)	9.02 (9.63)	0.12 (0.14)
O–Ala3	−0.65 (−0.66)	−0.86 (−0.96)	1.51 (1.62)	9.08 (9.74)	0.14 (0.18)	Coil	−0.70 (−0.72)	−0.85 (−0.91)	1.54 (1.63)	9.26 (9.81)	0.10 (0.12)
O–His4	−0.61 (−0.61)	−0.85 (−0.93)	1.45 (1.54)	8.72 (9.27)	0.17 (0.20)	Bend	−0.56 (−0.59)	−0.87 (−0.94)	1.42 (1.53)	8.54 (9.18)	0.22 (0.23)
O–His5	−0.57 (−0.55)	−0.88 (−0.98)	1.45 (1.53)	8.72 (9.21)	0.21 (0.28)	Bend	−0.57 (−0.59)	−0.92 (−0.99)	1.49 (1.57)	8.96 (9.44)	0.23 (0.25)
O–Ala6	−0.61 (−0.61)	−0.86 (−0.95)	1.47 (1.56)	8.84 (9.38)	0.17 (0.21)	Bend	−0.57 (−0.52)	−0.87 (−0.97)	1.44 (1.49)	8.66 (8.95)	0.21 (0.30)
O–Ala7	−0.61 (−0.61)	−0.87 (−0.97)	1.47 (1.58)	8.84 (9.49)	0.18 (0.22)	Coil	−0.43 (−0.44)	−1.03 (−1.10)	1.46 (1.54)	8.78 (9.28)	0.41 (0.43)
O–Asp8	−0.64 (−0.65)	−0.84 (−0.94)	1.48 (1.59)	8.90 (9.56)	0.14 (0.19)	Bend	−0.53 (−0.54)	−1.03 (−1.11)	1.56 (1.66)	9.38 (9.99)	0.32 (0.34)
O–Ala9	−0.62 (−0.61)	−0.87 (−0.99)	1.49 (1.60)	8.96 (9.61)	0.17 (0.23)	Bend	−0.64 (−0.64)	−1.03 (−1.10)	1.67 (1.74)	10.04 (10.47)	0.23 (0.26)
O–His10	−0.66 (−0.70)	−0.88 (−0.94)	1.54 (1.63)	9.26 (9.82)	0.14 (0.15)	Bend	−0.41 (−0.42)	−0.93 (−1.02)	1.34 (1.44)	8.06 (8.69)	0.39 (0.41)
O–His11	−0.72 (−0.76)	−0.86 (−0.92)	1.58 (1.68)	9.50 (10.13)	0.09 (0.09)	Coil	−0.43 (−0.44)	−1.07 (−1.14)	1.50 (1.58)	9.02 (9.52)	0.43 (0.44)
O–Ala12	−0.76 (−0.79)	−0.83 (−0.88)	1.58 (1.66)	9.50 (10.00)	0.04 (0.05)	Coil	−0.53 (−0.54)	−0.93 (−1.00)	1.46 (1.54)	8.78 (9.26)	0.27 (0.30)
O–Ala13	−0.68 (−0.72)	−0.91 (−0.98)	1.60 (1.70)	9.62 (10.23)	0.14 (0.16)	Coil	−0.46 (−0.51)	−0.92 (−0.97)	1.38 (1.48)	8.30 (8.89)	0.33 (0.31)

The calculated results out of parentheses are for 6–31+G* basis set, and those in parentheses SVP are for the basis set.

constant until 5.5 ns. After this time interval, the HB distance begins to increase leading to HB loss at both termini of the peptide and α-helix content decreases; thus, random coil and turn structure percentages increase. To investigate the influence of conformational effects on the EFG tensors at the site of backbone ^{17}O nuclei, initial α-helix and the final conformation derived from MD trajectory were considered in DFT calculations.

3.2. Computations of ^{17}O EFG tensors

Table 2 presents the calculated ^{17}O EFG tensors, C_Q and η_Q values for histidine, alanine and aspartic acid residues in initial α-helix backbone and MD simulated HRP II 169–181 conformations. It must be noted that since the NQR spectroscopy can be only studied in the solid state, we used the simulation in aqueous solution just for generating the different conformations of the peptide. These calculations were performed at the B3LYP/6–31+G* and B3LYP/SVP levels of theory. The EFG calculations indicate that the parameters calculated via 6–31+G* and SVP basis sets are practically coincident with each other. In following, we discuss the ^{17}O EFG calculations based on B3LYP/6–31+G* for initial and final conformations of HRP II 169–181 (His1-Ala 13).

Recent studies [29–31] have shown that ^{17}O EFG is very sensitive to geometry changes, and hydrogen-bonding interactions play a vital role in assigning NQR parameters in biological molecules, e.g. amino acids, nucleic acids, and small peptides. Furthermore, it must be noted that the residue type has no significant affect on EFG components of the main chain atoms [45]. For initial α-helix, oxygen atoms present in 1–9 residues are involved in hydrogen bonding (Table 1). So the electron distribution in these oxygen atoms should be dependent on HB length, bond angle and dihedral angle. The calculated C_Q value, for each oxygen nucleus are remarkably consistent and the maximum deviation from the average value (=8.87 MHz) is only 2.6%; corresponding to the O–Ala3. On the other hand, the calculated C_Q values for the remaining 10–13 residues are slightly larger than those of 1–9 residues, indicating that hydrogen hydrogen-bonding interactions cause a decrease in C_Q values. The calculated asymmetry parameters for all oxygen atoms in initial α-helix are almost small particularly for 10–13 residues. For example, C_Q (^{17}O–Ala13) is 0.78 MHz larger than C_Q (^{17}O–Ala6) and ^{17}O–Ala12 with η_Q=0.04 has smallest asymmetry parameter. The calculated average $C_Q(^{17}O)$=9.05 MHz for α-helix structure is consistent with those experimentally determined by Akihiro et al. [46], $C_{Q,exp}(^{17}O)$=9.28 MHz, and the theoretical value calculated by Torrent et al. [45], $C_Q(^{17}O)$=9.30 MHz. According to the results in Table 2, all C_Q (^{17}O) values change remarkably from the initial α-helix to the final structure. In N- and C-terminals, residues adopt coil structure while a bend secondary structure is present in middle residue. Moreover, it is found that oxygen atoms of middle residues (Ala6 and Ala7), His10 and Ala13 are involved in hydrogen hydrogen-bonding interactions of the final conformation (Table 1). For the O–His10, C_Q (^{17}O) value is decreased by 1.18 MHz and η_Q is increased from 0.14 to 0.39. This can be mainly attributed to formation of a proper hydrogen bond between O–His10 and N–Ala6 ($r_{O\ldots HN}$= 2.79 Å and ∠O···HN=158.84°) in final conformation. Due to the loss of hydrogen bonds for 1–3 residues and their conversion to coil structure, C_Q (^{17}O) is increased while an opposite trend is evidenced for 10–13 residues of C-terminal, which do not participate in HB of the initial structure.

4. Conclusion

The repeating sequence of malaria protein, HRP II 169–182, was studied in this paper via MD simulations and DFT calculations. Results indicated that coil and bend structures are dominant conformational forms in aqueous solution. DFT calculations revealed that ^{17}O EFG tensors depend on the conformation and HB interactions of the backbone. Thus, the converted quadrupole coupling constants show a significant sensitivity to the hydrogen bond interactions in peptide. The HB interaction causes a reduction in C_Q (^{17}O) of residues in two conformations. It was also concluded that asymmetry parameters of oxygen has small (<0.5) values in these conformations. These findings indicate the NQR spectroscopy measurement can be used to study peptide conformation, at least qualitatively. In the particular case of HRP II it might furthermore be useful to measure quadrupole tensors in the presence of heme as well, to test the possibility that the presence of heme induces alpha-helical structure in the peptides.

References

[1] V. Lemaître, M.E. Smith, A. Watts, A review of oxygen-17 solid-state NMR of organic materials—towards biological applications, Solid State Nucl. Magn. Reson. 26 (2004) 215–235.
[2] C.P. Slichter, Principles of Magnetic Resonance, Harper & Row, London, 1992.
[3] J.D. Graybeal, Molecular Spectroscopy, McGraw-Hill, Singapore, 1988.
[4] S.L. Chaplot, Parallelization in classical molecular dynamics simulation and applications, Comput. Mater. Sci. 37 (2006) 146–151.
[5] P. Ungerer, C. Nieto-Draghi, B. Rousseau, G. Ahunbay, V. Lachet, Molecular simulation of the thermophysical properties of fluids: from understanding toward quantitative predictions, J. Mol. Liq. 134 (2007) 71–89.
[6] M. Seibert, A. Patriksson, B. Hess, D. van der Spoel, Reproducible polypeptide folding and structure prediction using molecular dynamics simulations, J. Mol. Biol. 354 (2005) 173–183.
[7] W.L. Ash, M.R. Zlomislic, E.O. Oloo1, D.P. Tieleman, Computer simulations of membrane proteins, Biochim. Biophys. Acta 1666 (2004) 158–189.
[8] R.D. Schaeffer, A. Fersht, V. Daggett1, Combining experiment and simulation in protein folding: closing the gap for small model systems, Curr. Opin. Struck. Biol. 18 (2008) 4–9.
[9] H. Zhong, K.N. Kirschner, M. Leec, J.P. Bowen, Binding free energy calculation for duocarmycin/DNA complex based on the QPLD-derived partial charge model, Bioorg. Med. Chem. Lett. 18 (2008) 542–545.

[10] H. Goud, Y. Yanai, A. Sugawar, T. Sunazuka, S. Omura, S. Hirono, Computational analysis of the binding affinities of the natural-product cyclopentapeptides argifin and argadin to chitinase B from *Serratia marcescens*, Bioorganic Med. Chem. 16 (2008) 3565–3579.
[11] A. Barducci, R. Chelli, P. Procacci, V. Schettino, Misfolding pathways of the prion protein probed by molecular dynamics simulations, Biophys. J. 88 (2005) 1334.
[12] Y. Levy, E. Hanan, B. Solomon, O.M. Becker, Helix–coil transition of PrP106–126: molecular dynamic study, Protein 45 (2001) 382.
[13] A. Villa, A.E. Mark, G.A.A. Saracino, U. Cosentino, D. Pitea, G. Moro, M. Salmona, Conformational polymorphism of the PrP106–126 peptide in different environments: a molecular dynamics study, J. Phys. Chem. B 110 (2006) 1423.
[14] T.E. Wellems, R.J. Howard, Homologous genes encode two distinct histidine-rich proteins in a cloned isolate of *Plasmodium falciparum*, Proc. Natl. Acad. Sci. U. S. A. 83 (1986) 6065.
[15] http://www.rcsb.org/pdb/home/home.do.
[16] E.L. Schneider, M.A. Marletta, Heme binding to the histidine-rich protein II from *Plasmodium falciparum*, Biochemistry 44 (2005) 979.
[17] A.V. Pandey, R.M. Joshi, B.L. Tekwani, R.L. Singh, V.S. Chauhan, Synthetic peptides corresponding to a repetitive sequence of malarial histidine rich protein bind haem and inhibit haemozoin formation in vitro, Mol. Biochem. Parasitol. 90 (1997) 281–287.
[18] A.K. Rappé, E.R. Bernstein, Ab initio calculation of nonbonded interactions: are we there yet? J. Phys. Chem. A 104 (2000) 6117–6128.
[19] F. Sim, A. St-Amant, I. Papai, D.R. Salahub, Gaussian density functional calculations on hydrogen-bonded systems, J. Am. Chem. Soc. 114 (1992) 4391–4400.
[20] D.R. Hamman, Phys. Rev. B 55 (1997) 10157.
[21] S.S. Xantheas, Ab initio studies of cyclic water clusters $(H_2O)n$, $n = 1–6$. III. Comparison of density functional with MP2 results, J. Chem. Phys. 102 (1995) 4505–4517.
[22] J. Ireta, J. Neugebauer, M. Scheffler, On the accuracy of DFT for describing hydrogen bonds: dependence on the bond directionality, J. Phys. Chem. A 108 (2004) 5692–5698.
[23] S.J.A. Van Gisbergen, J.G. Snijders, E.J. Baerends, A density functional theory study of frequency-dependent polarizabilities and Van der Waals dispersion coefficients for polyatomic molecules, J. Chem. Phys. 103 (1995) 9347–9354.
[24] P. Salek, O. Vahtras, T. Helgaker, H. Agren, Density-functional theory of linear and nonlinear time-dependent molecular properties, J. Chem. Phys. 117 (2002) 9630–9645.
[25] H. Helgaker, P.J. Wilson, R.D. Amos, N.C. Handy, Nuclear shielding constants by density functional theory with gauge including atomic orbitals, J. Chem. Phys. 113 (2000) 2983–2989.
[26] J.R. Cheeseman, M.J. Frisch, F.J. Devlin, P.J. Stephens, Hartree–Fock and density functional theory ab initio calculation of optical rotation using GIAOs: basis set dependence, J. Phys. Chem. A 104 (2000) 1039–1046.
[27] K. Ruud, T. Helgaker, Optical rotation studied by density-functional and coupled-cluster methods, Chem. Phys. Lett. 352 (2002) 533–539.
[28] C. Cappeli, B. Mennucci, J. Tomasi, R. Cammi, A. Rizzo, The Cotton-Mouton effect of gaseous N-2, CO, CO2, N2OOCS and CS2: a density functional approach to high-order mixed electric and magnetic properties, Chem. Phys. Lett. 346 (2001) 251–258.
[29] H.J.C. Berendsen, J.P.M. Postma, W.F. van Gunsteren, J. Hermans, in: B. Pullman (Ed.), Intermolecular Forces, D. Reidel Publishing Company, 1981, p. 331.
[30] H.J.C. Berendsen, J.P.M. Postma, W.F. van Gunsteren, A. DiNola, J.R. Haak, Molecular dynamics with coupling to an external bath, J. Chem. Phys. 81 (1984) 3584–3590.
[31] B. Hess, J. Bekker, H.J.C. Berendsen, J.G.E.M. Fraaije, LINCS: a linear constraint solver for molecular simulations, J. Comp. Chem. 18 (1997) 1463–1472.
[32] K.A. Feenstra, B. Hess, H.J.C. Berendsen, Improving efficiency of large time-scale molecular dynamics simulations of hydrogen-rich systems, J. Comp. Chem. 20 (1999) 786–798.
[33] S. Miyamoto, P.A. Kollman, An analytical version of the SHAKE and RATTLE algorithms for rigid water models, J. Comput. Chem. 13 (1992) 952–962.
[34] U. Essmann, L. Perera, M.L. Berkowitz, T. Darden, H. Lee, L.G. Pedersen, A smooth particle mesh Ewald method, J. Chem. Phys. 103 (1995) 8577–8593.
[35] D. van der Spoel, E. Lindahl, B. Hess, G. Groenhof, A.E. Mark, H.J.C. Berendsen, GROMACS: fast, flexible, and free, J. Comput. Chem. 26 (2005) 1701.
[36] W.F. Van Gunsteren, S.R. Billeter, A.A. Eising, P.H. Hünenberger, P. Krüger, A.E. Mark, W.R.P. Scott, I.G. Tironi, Biomolecular Simulation: The GROMOS96 Manual and User Guide; vdf Hochschulverlag AG an der ETH Zürich and BIOMOS b.v.: Zürich, Groningen, 1996.
[37] M.J. Frisch, G.W. Trucks, H.B. Schlegel, G.E. Scuseria, M.A. Robb, J.R. Cheeseman, V.G. Zakrzewski, J.A. Montgomery Jr., R.E. Stratmann, J.C. Burant, S. Dapprich, J.M. Millam, A.D. Daniels, K.N. Kudin, M.C. Strain, O. Farkas, J. Tomasi, V. Barone, M. Cossi, R. Cammi, B. Mennucci, C. Pomelli, C. Adamo, S. Clifford, J. Ochterski, G.A. Petersson, P.Y. Ayala, Q. Cui, K. Morokuma, D.K. Malick, A.D. Rabuck, K. Raghavachari, J.B. Foresman, J. Cioslowski, J.V. Ortiz, A.G. Baboul, B.B. Stefanov, G. Liu, A. Liashenko, P. Piskorz, I. Komaromi, R. Gomperts, R.L. Martin, D.J. Fox, T. Keith, M.A. Al-Laham, C.Y. Peng, A. Nanayakkara, C. Gonzalez, M. Challacombe, P.M.W. Gill, B. Johnson, W. Chen, M.W. Wong, J.L. Andres, C. Gonzalez, M. Head-Gordon, E.S. Replogle, J.A. Pople, Gaussian 98, Gaussian Inc, Pittsburgh PA, 1998.
[38] R.G. Parr, W. Yang, Density-Functional Theory of Atoms and Molecules, Oxford Univ. Press, Oxford, 1989.
[39] A.D. Becke, Density-functional exchange-energy approximation with correct asymptotic behavior, Phys. Rev. A 38 (1988) 3089–3100.
[40] C. Lee, W. Yang, R.G. Parr, Development of the Colle-Salvetti correlation-energy formula into a functional of the electron density, Phys. Rev. B 37 (1988) 785–789.
[41] A. Schaefer, H. Horn, R. Ahlrichs, Fully optimized contracted Gaussian basis sets for atoms Li to Kr, J. Chem. Phys. 97 (1992) 2571–2577.
[42] R. Bersohn, Nuclear electric quadrupole spectra in solids, J. Chem. Phys. 20 (1952) 1505.
[43] P. Pyykkö, Spectroscopic nuclear quadrupole moments, Mol. Phys. 99 (2001) 1617–1629.
[44] W. Kabsch, C. Sander, Dictionary of protein secondary structure: pattern recognition of hydrogen-bonded and geometrical features, Biopolymers 22 (1983) 2577–2637.
[45] M. Torrent, D. Mansour, E.P. Day, K. Morokuma, Quantum chemical study on oxygen-17 and nitrogen-14 nuclear quadrupole coupling parameters of peptide bonds in alpha-helix and beta-sheet proteins, J. Phys. Chem. A 105 (2001) 4546–4557.
[46] T. Akihiro, S. Kuroki, I. Ando, T. Ozaki, A. Shoji, . Hydrogen-bonded structure and NMR parameters of oxygen-17 labeled poly(ι-alanine)s as studied by solid state oxygen-17 NMR spectroscopy, J. Mol. Struct. 442 (1998) 195.